LIFETIME PREDICTION FOR CERAMIC COMPONENTS SUBJECTED TO MULTIAXIAL LOADING

T. Thiemeier[1], A. Brückner-Foit[2], D. Munz[1,2]

The weakest-link model is generalized to allow the lifetime distributions of ceramic materials under complex loading conditions to be predicted. The necessary material parameters were determined by four point bending experiments (uniaxial stress state) and are used to predict the lifetime distribution for concentric double-ring tests (equibiaxial stress state). The prediction is compared with the lifetime distribution determined experimentally.

INTRODUCTION

Failure of ceramic materials is characterized by brittleness and a large amount of scatter in strength. This behaviour is due to a large number of very small flaws introduced in the manufacturing or machining processes. Unstable extension of one flaw described in linear elastic fracture mechanics will cause failure of the whole component. The failure stress depends on the size of the flaw initiating the fracture and must be described by statistical methods. The weakest-link model can be used for this purpose; it leads to a Weibull distribution of the material strength. In most ceramics, subcritical crack growth results in finite lifetimes, even under static loading conditions ("static fatigue"). Taking this factor into account, the weakest-link model produces a lifetime distribution. In the standard model, the effect of multiaxial loading is not considered. An extension of this model was introduced by Batdorf (1) and Evans (2) to describe the influence of multiaxiality on the strength distribution in materials. A generalization is presented of this extended model for the lifetime distribution of components subjected to multiaxial loading; it is compared with experimental results obtained on glass as a model material.

1) Institut für Zuverlässigkeit und Schadenskunde im Maschinenbau, University of Karlsruhe, Federal Republic of Germany

2) Institut für Material- und Festkörperforschung IV, Nuclear Research Center, Karlsruhe, Federal Republic of Germany

WEAKEST LINK MODEL

First, only inert failure is considered, i.e. failure without subcritical crack growth. The flaws are assumed to be uniformly distributed in the volume and on the surface, respectively. Subsequently, only surface flaws will be taken into account; the extension for volume flaws is straightforward. The size of each flaw is characterized by its critical stress, σ_c. The failure probability, $dP_{f,dA}$, of a surface element, dA, is proportional to dA and depends on the local stress, σ. Under the assumption of component failure in case one surface element fails, the failure probability of the component is given by

$$P_f = 1 - exp\left[- \int_A dP_{f,dA} \right] \quad . \tag{1}$$

P_f depends on the size of the stressed surface. For the failure probability, $dP_{f,dA}$, of the surface element, dA, the expression

$$dP_{f,dA} = \frac{1}{A_o} \left(\frac{\sigma}{\sigma_o} \right)^{m_c} dA \tag{2}$$

is used. σ_0 and m_c are parameters characterizing the flaw population, which must be determined experimentally. A_0 is a reference area. From eqs. (1) and (2) follows

$$P_f = 1 - exp\left[- \frac{1}{A_o} \int_A \left(\frac{\sigma}{\sigma_o} \right)^{m_c} dA \right] \quad . \tag{3}$$

In general, σ depends on the location. If a reference stress, σ^*, is used to characterize the component stress (e.g. the outer fibre stress in the case of bending), Eq. (3) can be written as a Weibull distribution of the failure stress σ_c^*:

$$P_f = P[\sigma_c^* \leq \sigma^*] = 1 - exp\left[- \left(\frac{\sigma^*}{b_c} \right)^{m_c} \right] \tag{4}$$

$$with \qquad b_c = \left[\frac{1}{A_o} \int_A \left(\frac{\sigma / \sigma^*}{\sigma_o} \right)^{m_c} dA \right]^{\frac{-1}{m_c}} \tag{5}$$

CONSIDERATION OF MULTIAXIAL LOADING

Up to now the local stress has been treated as a scalar quantity (σ). For multiaxial stress states to be taken into account, the surface flaws are modeled as plane cracks normal to the surface. Their size can be expressed by their critical mode I stress,

$$\sigma_{Ic} = \frac{K_{Ic}}{Y_I \sqrt{a}} \quad . \tag{6}$$

Their orientation in the stress field is described by the orientation angle, ϕ (Fig. 1). All orientations are assumed to have the same probability. With the angle of orientation, ϕ, and the stress tensor, $\underline{\sigma}_{ij}$, known, the normal stress, σ_n, and the shear stress, τ, acting on the crack plane can be evaluated easily. A crack geometry model and a multiaxial failure criterion allow an equivalent mode I stress, σ_{Ieq}, to be calcu--

lated (Fig. 2). With σ_{Ieq}, the failure probability of the surface element, dA, is expressed as in Eq. (2), but ϕ occurs as an additional variable. As all orientations are assumed to be of the same probability, the average of all possible angles must be taken:

$$dP_{f,dA} = \frac{1}{2\pi} \int_{\phi=0}^{2\pi} \frac{1}{A_o} \left(\frac{\sigma_{Ieq}(\underline{\sigma}_{ij}, \phi)}{\sigma_{Io}} \right)^{m_c} d\phi \; dA \tag{7}$$

Again, σ_{Io} and m_c are parameters of the crack population to be determined experimentally. A combination of Eq. (7) and Eq. (1) leads to a Weibull distribution of the failure stress (Eq. (4)), but with a different expression for b_c:

$$b_c = \left[\frac{1}{A_o} \int_A \frac{1}{2\pi} \int_{\phi=0}^{2\pi} \left(\frac{\sigma_{Ieq}/\sigma^*)}{\sigma_{Io}} \right)^{m_c} d\phi \; dA \right]^{\frac{-1}{m_c}} \tag{8}$$

CRACK GEOMETRY MODELS

As the real crack geometry is not known, a crack model as realistic as possible must be selected and the correction functions, Y_I, Y_{II}, Y_{III}, necessary to calculate σ_{Ieq} must be known. Three crack models have been used:

(a) Through-wall crack ("Griffith crack"),

(b) penny-shaped crack,

(c) semicircular surface crack.
For this geometry, only K_I is known (Newman and Raju (3)). K_{II} and K_{III} are estimated on the assumption that, compared to the penny-shaped crack, the effect of the surface can be taken into account by the same factor for all three modes. In mode I, the factor is determined to be 1.03.

FAILURE CRITERIA

Two failure criteria are used (mode III was neglected):

(a) Criterion of the energy release rate, G:

$$G_c \leq G = \frac{1-\nu^2}{E} (K_I^2 + K_{II}^2)$$

$$\sigma_{Ieq} = \sqrt{\sigma_n^2 + \tau^2 (Y_{II}/Y_I)^2} \tag{9}$$

(b) Criterion according to Richard (4)

$$\sigma_{Ieq} = \frac{1}{2}\sigma_n + \frac{1}{2}\sqrt{\sigma_n^2 + (2 \cdot a_1 \cdot \tau)^2 (Y_{II}/Y_I)^2}, \quad a_1 = \frac{K_{Ic}}{K_{IIc}} \tag{10}$$

This is an empirical criterion.

Both criteria are shown in a K_{II}/K_{Ic}-K_I/K_{Ic}-diagram in Fig. 3. Fig. 4 shows curves of the same failure probability in an dimensionless principal-stress diagram for $m_c = 14$. For this, Eq. (7) was used.

EXTENSION TO LIFETIME DISTRIBUTIONS

In the following section subcritical crack growth is taken into account. For many ceramic materials and glass, the relation between crack velocity and K_I can be described by a power law:

$$da/dt = A \cdot K_I^{\ n} \tag{11}$$

A and n are parameters characterizing the subcritical crack growth rate, which depend on the material and the environment. If it is assumed that a multimodally loaded crack will expand at the same velocity as a crack under a mode I loading condition with σ_{Ieq}, Eq. (11) results in the following expression for the lifetime, t_f, under a constant load (Ritter (5)):

$$t_f = B(A, K_I, n, Y_I) \cdot \sigma_{Ic}^{(n-2)} \cdot \sigma_{Ieq}^{(-n)} \tag{12}$$

The parameter, B, can be evaluated directly by experiments (5). Eq. (12) represents a unique relation between σ_{Ic} and t_f for a given σ_{Ieq}. Therefore, Eq. (7), furnishing the probability that dA contains a flaw with $\sigma_{Ic} \leq \sigma_{Ieq}$, can be transformed into an expression of the probability of the lifetime of dA being less than a given time t:

$$dP_{dA}[t_f \leq t] = \frac{1}{2\pi} \int_{\phi=0}^{2\pi} \frac{1}{A_o} \left(\frac{t}{B \cdot \sigma_{Io}^{(n-2)} \cdot \sigma_{Ieq}^{(-n)}} \right)^{\left(\frac{m_c}{n-2}\right)} d\phi \tag{13}$$

Substituting $dP_{f,dA}$ in Eq. (1) by $dP[t_f \leq t]$ results in a Weibull distribution for the lifetime, t_f, of the component:

$$P[t_f \leq t] = 1 - exp\left[-\left(\frac{t}{b_t} \right)^{m_t} \right] \tag{14}$$

$$m_t = \frac{m_c}{n-2} \quad , \quad b_t = \left[\frac{1}{A_o} \int_A \frac{1}{2\pi} \int_{\phi=0}^{2\pi} \left(\frac{1}{B \cdot \sigma_{Io}^{(n-2)} \cdot \sigma_{Ieq}^{(-n)}} \right)^{m_t} d\phi dA \right]^{\frac{-1}{m_t}} \tag{15}$$

EXPERIMENTS

Experiments with glass as a model material were performed on two test geometries, which produce different stress states in the specimens:

(a) Four point-bending (Fig. 5a) In the area between the inner rollers the bending moment is constant (uniaxial stress state).

(b) Concentric double-ring test (Fig. 5b)
The maximum stresses occur in the area within the inner ring. Both radial and tangential stresses are constant and equal (equibiaxial stress state).

TABLE 1 - Parameters of measured lifetime distributions
(m_t,b_t - Weibull parameters, $E(t_f)$ - mean value of t_f)

loading case	σ^* [MPa]	m_t	b_t [h]	$E(t_f)$ [h]
4-point bending	42.0	1.8	0.40	0.35
"	43.5	1.3	0.33	0.30
"	45.0	1.15	0.21	0.20
"	48.0	1.4	0.1	0.10
double-ring	35.0	1.35	0.23	0.21

For both geometries, the maximum outer fibre stress was used as the reference stress σ^*. The parameters of the inert strength distribution (Eqs. (4),(8)) were evaluated in a test series under four point-bending; subcritical crack growth was suppressed by a very high loading rate (1000 MPa/s) in an air environment:

$$m_c = 14 \qquad b_c = 110.5\ MPa \tag{16}$$

Fig. 6 shows the measured inert strengths and the fitted Weibull distribution in a Weibull diagram (because of the distortion of the axes, Weibull distributions become straight lines). Additional test series were performed under static loads in water; water increases the crack velocity in glass by several orders of magnitude. The lifetime distributions for four stress levels (four point-bending) were evaluated (Table 1, Fig. 7). The crack growth parameters, n and B, were calculated from the observed dependency between the distribution parameter, b_t, and the reference stress, σ^*:

$$n = 10.5 \qquad B = 760\ s\ MPa \tag{17}$$

Lifetime tests were performed under the same conditions with the double-ring equipment (Fig. 8). In spite of the low stress level (σ^* = 35 MPa), the mean lifetime was rather short, compared to the mean lifetimes measured in four point-bending (Table 1). Under the assumption of Griffith's crack model and Richard's failure criterion, with $a_1 = 0.5$ the parameter, b_t, of the double-ring lifetime distribution with σ^* = 35 MPa was predicted with Eq. (5) (no effect of multiaxiality included) and with Eq. (8). The results are compared with the experimental values in Table. 2.

TABLE 2 - Comparison of predicted and experimental results for the double-ring lifetime distribution with σ^* = 35 MPa

m_t, b_t - Weibull parameters $E(t_f)$ - mean-value of t_f	m_t	b_t [h]	$E(t_f)$ [h]
theory			
without multiaxiality (Eq.(5))	1.7	1.25	1.12
with multiaxiality (Eq. (8))	1.7	0.41	0.37
experiment(Fig. 8)	1.4	0.23	0.21

DISCUSSION

There are two reasons for the average lifetime under double-ring loading conditions being shorter than under four point-bending conditions:

(1) The loaded area is larger in the double-ring geometry used. Therefore, the probability of a large flaw occurring is increased. This effect is included both in Eq. (5) and in Eq. (8).

(2) Because of the equibiaxial stress state in double-ring loading, all crack planes are loaded in mode I. In four point-bending, cracks oriented parallel to the principal stress are not loaded. This difference is included only in Eq. (8) and results in a lower value being predicted for the average lifetime.

The prediction by Eq. (8) and the experiment differ by a factor of 1.8 . Considering the large amount of scatter typical of lifetime distributions, this is not too bad a result. The error in the prediction by Eq. (5) is much larger (factor 5.3). It is planned to improve the model by using more realistic crack geometries and failure criteria.

REFERENCES

(1) Batdorf, S.B., "Fundamentals of the Statistical Theory of Fracture," Proc. Int. Symp. on Fracture Mechanics of Ceramics, Vol. 3, "Flaws and Testing," Ed. by R.C.Bradt, D.P.H.Hasselman and F.F.Lange, Plenum Press, New York, USA, 1977, pp. 1-30.

(2) Evans, A.G., J. Am. Ceram. Soc., Vol. 61, 1978, pp. 302-308.

(3) Newman, J.C. and Raju, J.S., Eng. Fract. Mech., Vol. 15, 1981, pp.185-192

(4) Richard, H.A., "Bruchvorhersagen bei überlagerter Normal- und Schubbeanspruchung von Rissen," VDI-Forschungsbericht 631/85, VDI-Verlag, FRG, 1985.

(5) Ritter, J.E., Jr., "Engineering Design and Fatigue Failure of Brittle Materials," Proc. Int. Symp. on Fracture Mechanics of Ceramics, Vol. 4, "Crack Growth and Microstructure," Ed. by R.C.Bradt, D.P.H.Hasselman and F.F.Lange, Plenum Press, New York, USA, 1978, pp. 667-686.

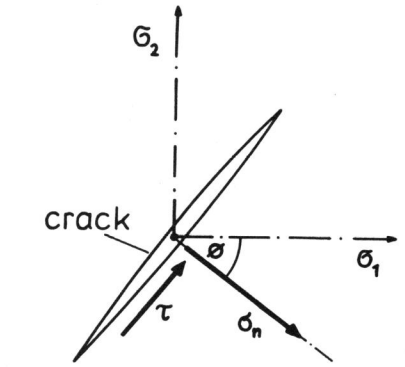

Figure 1: Surface crack in the stress field

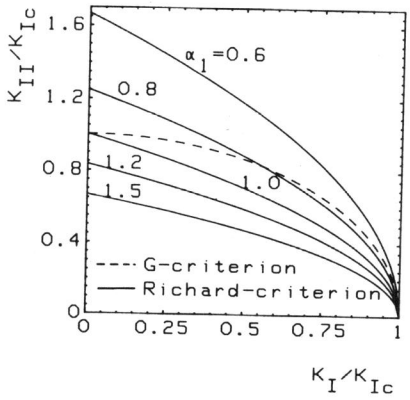

Figure 3: K_{II}/K_{Ic}-K_I/K_{Ic}-diagram for the failure criteria used

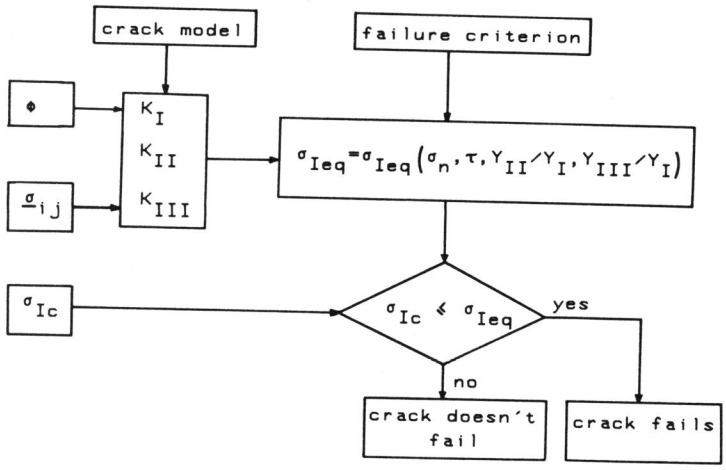

Figure 2: Flow chart for the determination of σ_{Ieq}

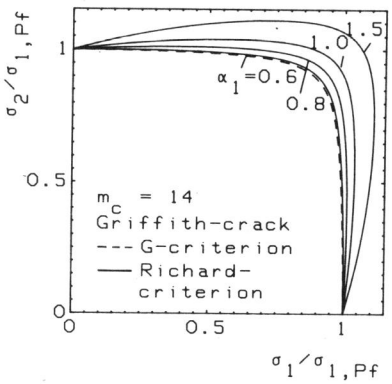

Figure 4: Curves of the same failure probability

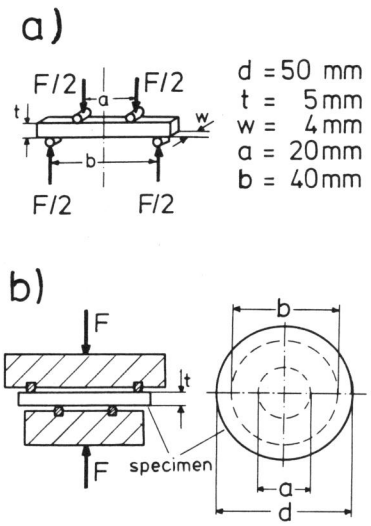

Figure 5: (a) Double-ring geometry
(b) 4-point bend geometry

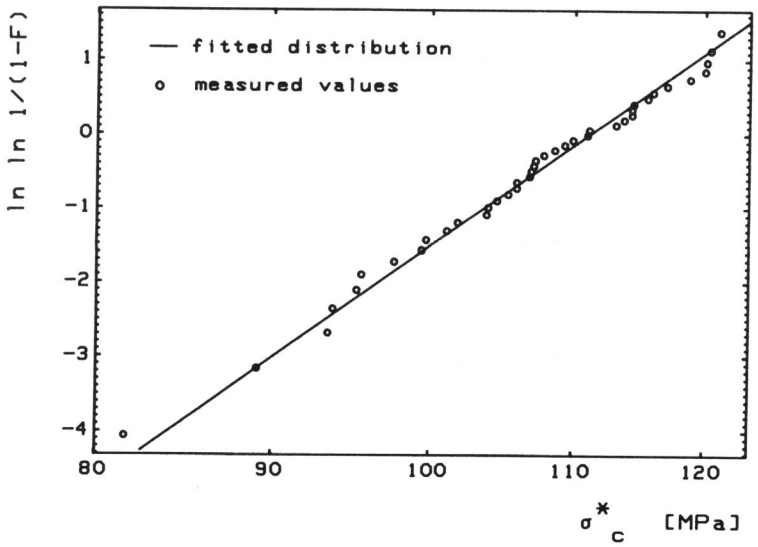

Figure 6: Weibull diagram of the inert strength distribution (four-point bending)

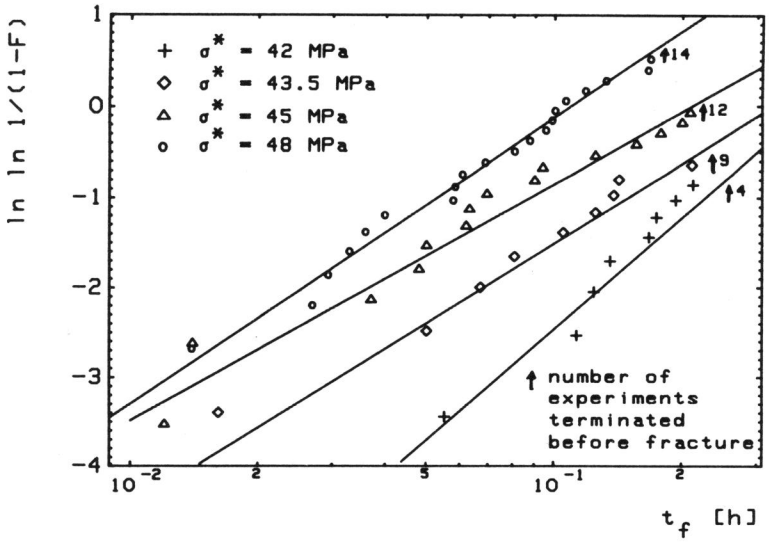

Figure 7: Weibull diagram of the lifetime distributions (four-point bending)

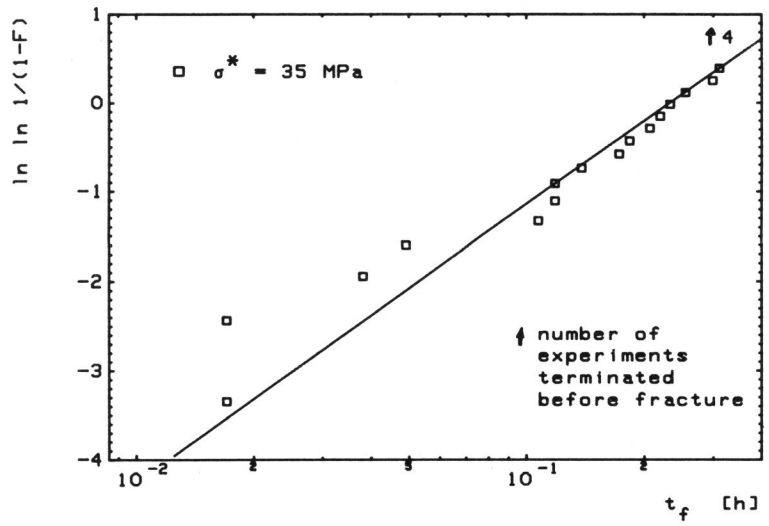

Figure 8: Weibull diagram of the lifetime distribution (double-ring)